Materials Science Forum
ISSN: 1662-9752, Vol. 1004, pp 479-489
doi:10.4028/www.scientific.net/MSF.1004.479
© 2020 The Author(s). Published by Trans Tech Publications Ltd, Switzerland.
Submitted: 2019-08-09
Revised: 2020-02-10
Accepted: 2020-02-19
Online: 2020-07-28

Evolution of SiO_x Shell Layers on SiC-SiO_x Core-Shell Nanowires

Andrea Broggi[1,a*], Eli Ringdalen[1,b] and Merete Tangstad[1,c]

[1]Alfred Getz vei 2b, 7034 Trondheim, Norway

[a]andrbrog@ntnu.no, [b]eli.ringdalen@sintef.no, [c]merete.tangstad@ntnu.no

Keywords: Nanowires; mechanism of formation; melting-point depression; characterization, silicon suboxide

Abstract. Composite core-shell SiC-SiO_x nanowires can be produced by heating quartz and SiC powders, with addition of Ar(g) or He(g). The two powders are mixed to create pellets, which will react to SiO(g) and CO(g) at elevated temperatures. The two gases will react on a colder surface, producing a web of SiC-SiO_x nanowires. The product serves as a precursor for SiC nanowires production. During the process, silicon and oxygen accumulate at high energy points, forming SiO_x nodules. Nodules can either generate in proximity of stacking faults, or where two or more nanowires are close to each other. The present work investigates the role of crystal defects in the wettability between silica and silicon carbide. Samples were collected and analyzed under Scanning Electron Microscopy (SEM) and Transmission Electron Microscopy (TEM). The results show that β-SiC grows mainly in the [111] direction. Crystal defects are located in the SiC core-phase. SiO_x initially develops a uniform layer as thick as the core-phase itself. SiO_x nodules would first form where the defects are present, by accumulating at high energy sites. Droplets on a flat surface imply poor wettability. The mechanism of formation of the nodules is compared to two earlier proposed theories. In conclusion, the wettability of SiO_x and SiC at nanoscale is controlled by the presence of crystallographic defects. Continuous SiO_x layers and bead-like structures can be found in the same temperature interval. The microstructural changes depend on the local energy balance.

Introduction

SiC nanowires are used for a wide number of applications, which can combine the mechanical properties of SiC and the nanosized confinement effect on electrons. SiC nanowires are used for reinforcement in epoxydic or rubber materials, as well as for light-emitting devices [1,2].

A simple method to produce nanostructured-SiC has been tested by many authors, in a wide temperature and pressure range. The method consists in mixing and heating powders of SiO_x, Si, C or SiC, in presence of argon or helium. A carbon-containing gas species can also act as carbon source in the system. Once the powders have reacted, SiC-SiO_x nanowires are formed. SiO_x can be leached by HF treatment [3]. The final product will be clean, long and multi-crystalline SiC nanowires.

The SiC-SiO_x nanowires have been characterized and reported by a number of works. Many are related to the world of nanotechnology [4–17], but few of them were also related to the industrial production of silicon [18–22]. SiO(g) and CO(g) are respectively an intermediate and a by-product in silicon production, hence the importance of studying the reaction between these two gases.

TEM analysis showed that the SiC nanowires were either covered with a bead-structured layer, or with a uniform SiO_x coating. The structures could be noticed at the same time in different temperature areas, or even in the same sample [18,19,22]. Many works suggest a correlation between crystal defects and SiO_x-microstructure in the nanowires [5,7–10,12,13,16,17,23–25].

Some studies propose mechanisms of formation for the SiO_x nodules in nanowires. Wei et al. [11] and Wu et al. [12] proposes a transformation from the beads to a uniform layer. Beads would grow at stacking faults of the SiC core-phase. Surface tension will stabilize the SiO_x coating, by spreading it on the SiC surface. However, Liu et al. [10] proposes a mechanism which works exactly in the opposite way. First, a uniform SiO_x-layer grows together with the SiC core-phase. Once unstable, the coating decreases its interface energy by creating spheres, especially in correspondence of stacking faults in SiC nanowires.

This article is an open access article under the terms and conditions of the Creative Commons Attribution (CC BY) license (https://creativecommons.org/licenses/by/4.0)

The aim of this work is to study the nodule formation mechanism and the changes in morphology of the SiO_x phase. Nanowires are produced and investigated by SEM and TEM. The contact angle between SiO_x nodules and SiC will be specifically studied.

Experimental

The experimental procedure is reported in Broggi et al. [22,26]. Quartz (99 wt.% SiO_2, a commercial product called Quartz20) and SiC powders (>95 wt.% SiC, produced by Washington Mills) were mixed with water to make pellets with diameters between 1-2 mm. Table 1 shows the powders size distribution of the initial materials. The parameters d_{10}, d_{50} and d_{90} are used to describe the particle size distribution. They are respectively defined as the diameter when the accumulated percentage in the particle size distribution of each material is 10%, 50% and 90%. Pellets were all made by the same batch of powder. The final mixture has a composition of SiO_2 : SiC = 2 : 1 molar ratio.

A graphite tube furnace was used to produce SiO(g) and CO(g) and collect SiC-SiO_x nanowires. The equipment is divided into two parts: a reaction chamber, located at the top, and a gas production chamber at the bottom. An overview of the system is given in Fig. 1. The bottom crucible contains 20 g of pellets. SiO(g) and CO(g) generate by heating the pellets to a target temperature and holding it for a fixed time. The reaction occurring is

$$2\ SiO_2\,(s) + \ SiC\ (s) \rightarrow 3\ SiO(g) + CO(g) \qquad (1)$$

An alumina tube goes through the whole setup down to the gas production chamber. Its function is to transport of Ar(g) or He(g) to the gas production chamber. Helium was chosen after noticing damages on the furnace, caused by argon ionization [26,27]. The reaction chamber is a 25-mm wide and 150-mm high open cylinder. Graphite wool further insulates the system. The chamber contains SiC particles, on which the nanowires are produced. A C-type thermocouple is shielded by the tube and placed at different positions in the chamber. This was done to assess a temperature gradient in the reaction chamber.

The furnace was purged with He(g) before starting, and the pressure was reduced to 180 mTorr, before injecting inert gas at 1 atm. While producing SiO(g) and CO(g) at elevated temperatures, the pressure in the reaction chamber ranged between 1.4-1.6 atm.

The parameters changed through the experimental plan were the inert gas flow, the SiC particle size in the reaction chamber, the target temperature and holding time. Ar or He were used at flow rates of 0.02, 0.1 and 0.4 l/min. Target temperature at the gas production chamber was held at 2000°C, holding times at 0.5, 1 and 4 hours. Experiments at 0.02 l/min and 0.4 l/min and 1 hour holding time have been repeated 5 times each, to confirm reproducibility.

All the experiments gave SiC-SiO_x nanowires in different amounts but showing the same microstructures. Further information about mass balance and temperature gradient assessment is given in Broggi et al. [22,26].

Table 1: Size parameters for powders used to produce pellets

Powder	d_{10} [µm]	d_{50} [µm]	d_{90} [µm]
Quartz20	1.700	10.73	58.38
SiC	0.179	0.955	1.876

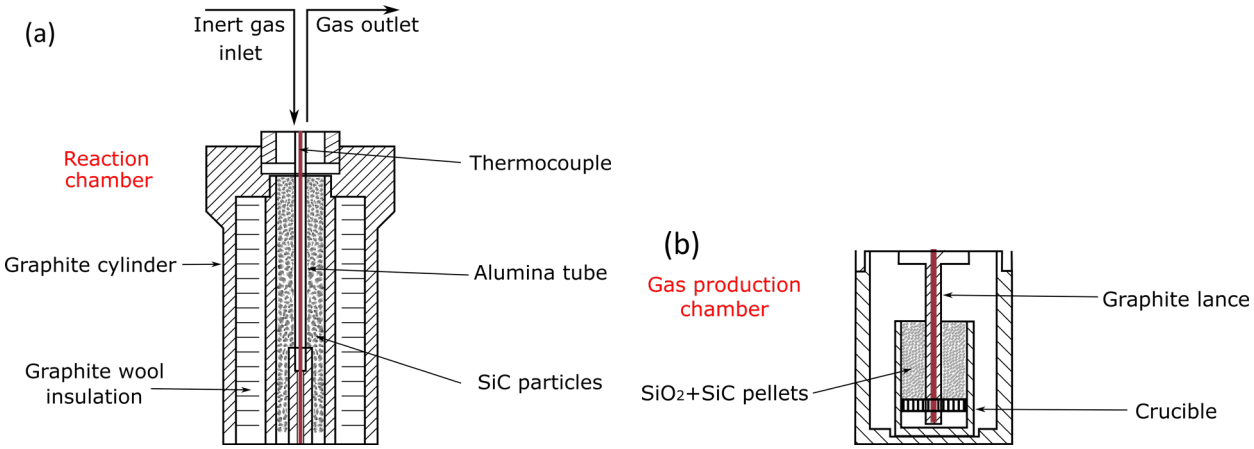

Fig. 1: a) Reaction chamber; b) Gas production chamber

Back-scattered (BSE) and secondary-electron (SE) images were taken with a Hitachi SU-6000 FE-SEM. The working distance was set at 15 mm and the voltage between 5 and 20 kV. SiC particles were analyzed as-fabricated. Other particles were mounted in traditional epoxy, to focus on morphology and composition. The application of a 20-nm thick carbon coating grants the conductivity of the epoxy, which is necessary for SEM analysis.

Samples were collected from one the experiments with 1 hour holding time and 0.02 l/min injected Ar flow, for the TEM preparation. Thin and soft layers of nanowires were scratched from the SiC condensation particles. The samples that scratched out were then mixed in an isopropanol solution. A droplet of solution containing the sample was extracted and applied on a copper TEM sample grid. The sample was finally dried at room temperature.

TEM was performed with a double Cs corrected coldFEG JEOL ARM 200F, operated at 200kV and equipped with a large solid angle (0.98 sr) Centurio SDD detector for X-ray energy dispersive spectroscopy (EDS) and a Quantum ER GIF for Electron Energy Loss Spectroscopy (EELS). Pictures collected from TEM analysis were scanned by High Angle Annular Dark Field Scanning Transmission Electron Microscopy (HAADF-STEM) and Selected Area Diffraction Analysis in Bright Field (SADA-BF). Contact angles were measured by using the software ImageJ®.

Results

The SEM analysis shows that the reaction product appears as an intricated web of very thin wires, with nodules occasionally formed in different positions. The configuration is shown in Fig. 2. When nanowires generate at colder temperatures in the reaction chamber (1150-1250°C) [22], the compound covers the SiC substrates as a blue layer. By looking at the layer in SEM, wires are present, and nodules appear in low numbers. Nanowire size ranges between 20-80 nm. [22].

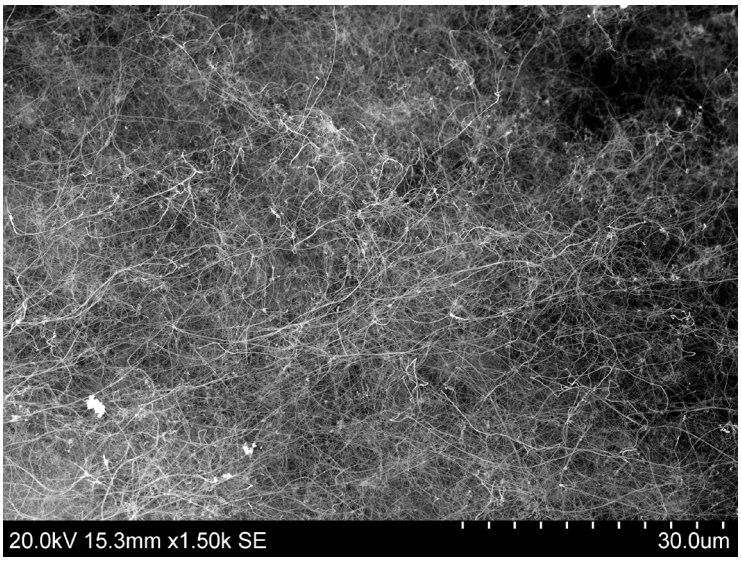

Fig. 2: SEM picture of blue layer. SiC-SiO_x nanowires poor in nodules (1150-1250°C)

When temperature increases in the reaction chamber (1250-1750°C), the SiC particles are covered in a white, thicker layer. Nanowires production increases at higher temperatures [22]. Nanowire forests produced at higher temperatures are richer in nodules. This was also noticed by Hu et al. [8,9]. Mølnås [18] analyzed the phenomenon in the temperature range between 1311-1425°C. Nanowires size range between 50-100 nm in diameter, whereas nodules can have diameters up to 1 μm [22]. Fig. 3 shows the morphology of the white nanowires forest.

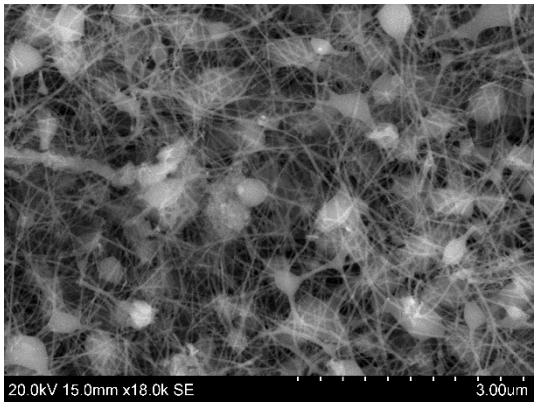

Fig. 3: SEM picture of white layer SiC-SiO_x nanowires rich in nodules (1250-1750°C)

Stacking faults in SiC nanowires are seen both in blue and white sample. They can be recognized in Fig. 4 and Fig. 5 as the darker transversal marks in the core-phase of the nanowires. A Fourier-Transformed diffractogram revealed a [111] growth direction for the SiC core-phase. The plane spacing in the crystalline domains is 2.2 Å. This value corresponds to the β-SiC polytype, also known as 3C-SiC.

The shell phase, made of SiO_x, is always seen as amorphous, because of its interaction with the TEM voltage. The core phase diameter makes about one third of the total nanowire diameter, when the SiO_x coating is uniform.

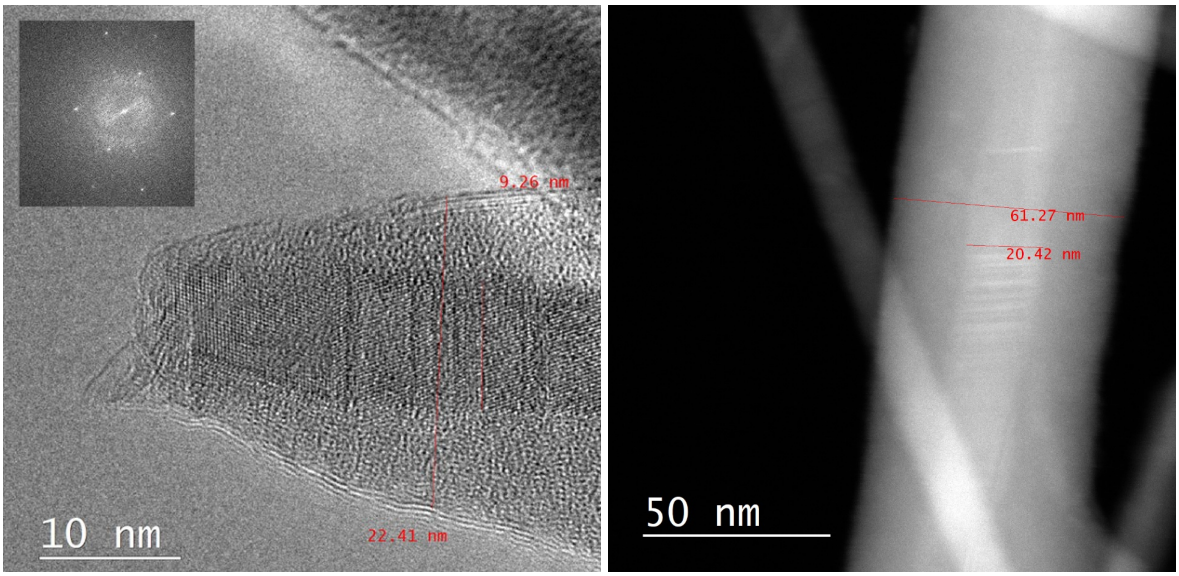

Fig. 4: Left: Core and shell phase diameters in uniform coating configuration, with Fourier-Transformed diffractogram at top left corner. Right: Diameter of core and shell-phases in uniform coating configuration. Grey transversal lines in the core-phases are stacking faults of SiC nanowires. T = 1280-1500°C

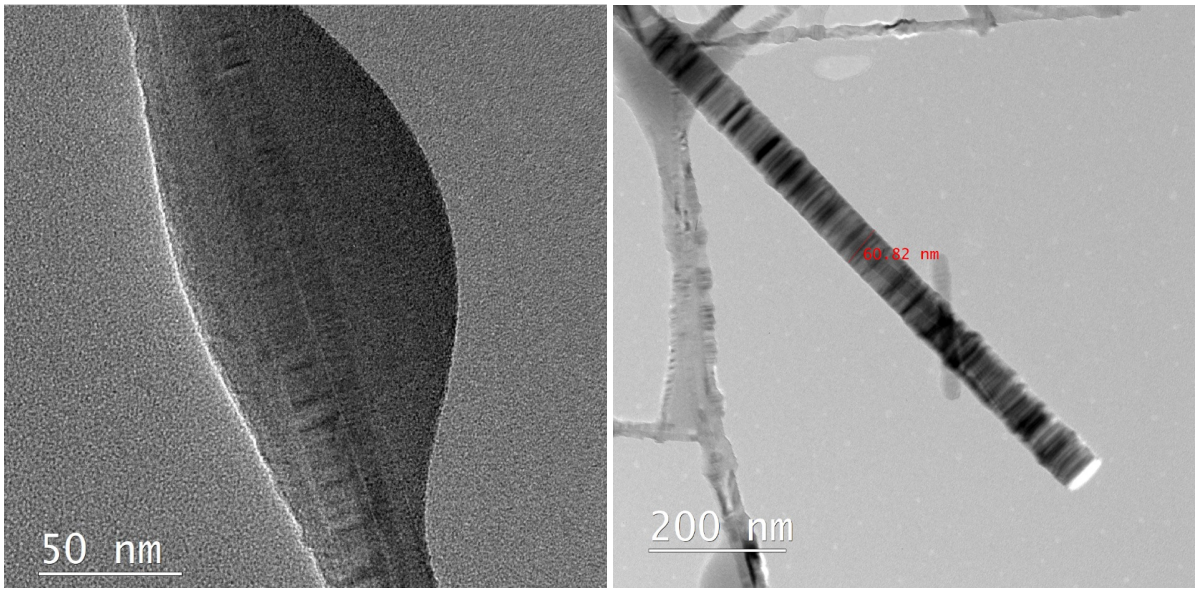

Fig. 5: Stacking faults in correspondence of a nodule (left) and on a naked nanowire rich in stacking faults (right), T = 1500-1580°C

The shell-phase changes its morphology, according to local temperature and position. Nodules are either randomly distributed (Fig. 6), or organized into bead-structures [7,23] (Fig. 7), as found in samples from experiments with 0.02 and 0.4 l/min injected He. SiO_x can either coat the nanowires uniformly or leave some nanowires uncoated (Fig. 8). Uniform coating is easier to find at lower temperatures. Uncoated SiC wires and nodules are more common at higher temperatures.

Uncoated wires can be recognized by TEM. They are thinner than SiO_x-coated wires. The contrast between SiO_x and SiC is easily noticed, as the TEM signal passes through the sample and reveals the interfaces between the two phases. The bubble-shaped light grey areas are organic contaminations from the TEM substrate grid.

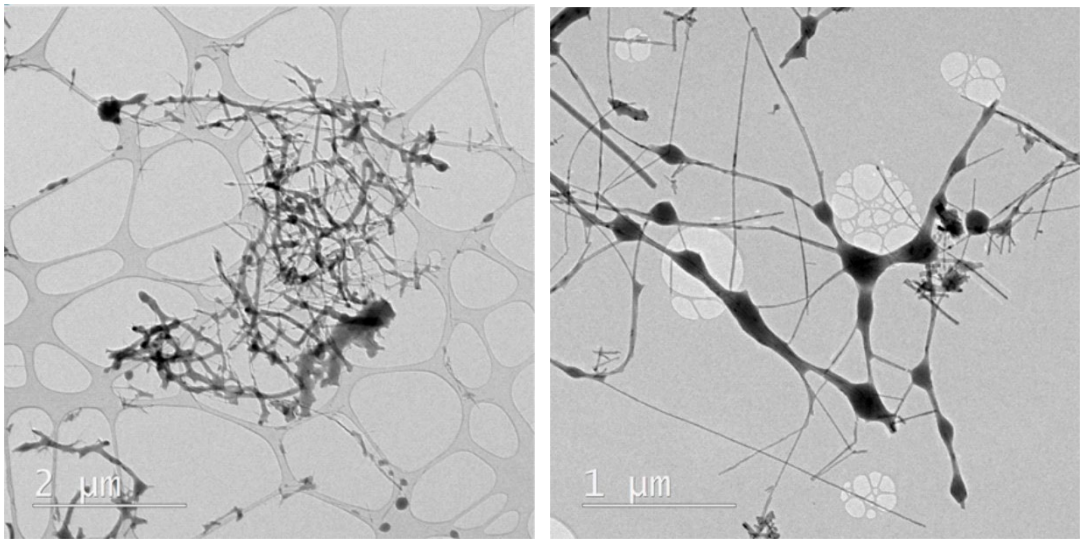

Fig. 6: Left: TEM image overview of blue sample (T=1280-1500°C); Right: TEM image of white sample (1500-1580°C)

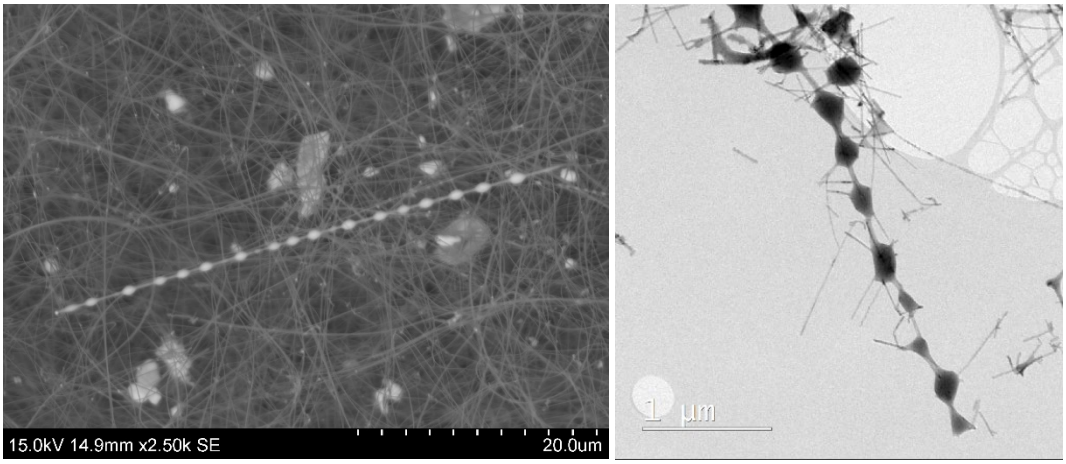

Fig. 7: Left: SE-SEM image of a bead structure, experiment at 0.4 l/min He and 1 hour holding time, T = 1180-1200°C; Right: TEM image of a bead structure, T = 1500-1580°C

More pictures were taken on some of the nodules, to assess the contact angles between the core and the shell phase (Fig. 8). Contact angles were also collected from Fig. 7 (right) and 6 (right). Contact angles were also measured for the bead structures, for both white and blue samples. 12 measurements were taken in the blue sample, whereas 30 were analyzed in the white layer. Both these samples were collected from the same experiment with 0.02 l/min injected Ar flow and 1 hour holding time at 2000°C. The contact angle is defined as the angle between a SiC-core external surface, and the tangent line to the oxide shell-phase. A lower contact angle corresponds to a higher wettability, i.e. SiO_x coats uniformly the layer. A contact angle close to 90° corresponds to a weaker wettability of SiO_x on SiC.

The areas with the uniform coating are more common for the blue sample. However, where the nodules form, the contact angle is assuming a similar value. Since it was easier to see the interface, the supplementary angle to the contact angle was measured. To find the real contact angle, it will be enough to subtract the measured angle from 180°. The results gave a contact angle of 43.6±9.9°, for both white and blue layer.

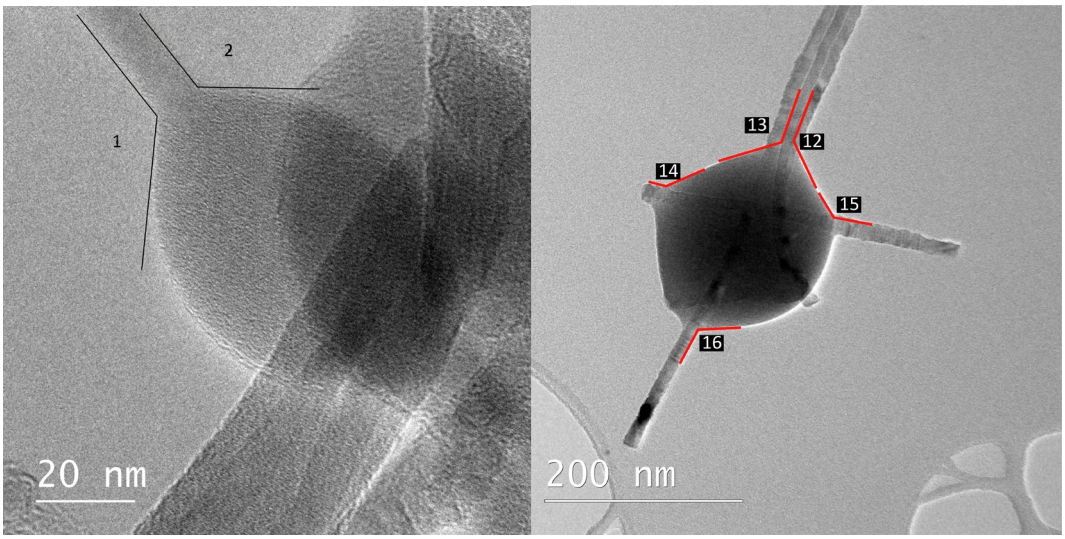

Fig. 8: Contact angle measurements. Left: blue sample; Right: white sample (right). There is a SiC which is not coated with SiO_x, at the right side of the nodule

Discussion

Mechanism of formation of nodules. Liu et al. [10], Wei et al. [11] and Wu et al. [12] proposed mechanisms of formation of the SiO_x nodules between the wires. The first two support a transformation of silica from a uniform layer to bead-structures, whereas the last proposed a beads-to-layer mechanism. These theories present good intuitions, but also relevant conceptual flaws, as will be discussed in the following. A new mechanism for beads formation must be proposed. The proposed mechanism is sketched in Fig. 9.

First, a continuous SiO_x-coating is generated around the SiC-core phase. This assertion supports the layer-to-bead (LTB) mechanism proposed by Liu et al. [10], but it also respects the mass balance of a chemical reaction. SiO_x must generate at the same time with SiC, when SiO(g) and CO(g) meet the condensation surface. According to Wu's beads-to-layer mechanism (BTL), SiO_x would grow on the defects of SiC nanowires. The BTL mechanism implies that SiC develops as nanowires first, and then SiO_x generates on the SiC nanowires from the gas phase. However, the reaction thermodynamics specify that SiC and SiO_x must generate at the same time, since they are the products of reaction (-1). This reaction number is chosen, as it is the opposite reaction happening to the SiO_2-SiC pellets in the gas production chamber.

$$3\ SiO(g) + CO(g) \rightarrow 2\ SiO_2(s) + SiC(s) \qquad (-1)$$

The compounds will assemble into coated nanowires from the adhesion site with the substrate [28].

Defects can periodically be present or uniformly spread in SiC nanowires. Hu et al. [8] suggests that oxygen inclusions may be responsible of the crystalline defects in the SiC wires. The partial pressure of oxygen should be very low in this work, thanks to the vacuuming procedure. The partial pressure of oxygen can be estimated from the equilibrium between SiO(g) and O_2(g) in the reaction

$$2\ SiO(g) + O_2(g) = 2\ SiO_2(s) \qquad (2)$$

Given a partial pressure of SiO(g) of 0.75, the equilibrium partial pressure of oxygen at 1150°C and 1800°C can be calculated for reaction (2). The temperature dependence of the equilibrium constants K_{eq} for Reaction (2) is found from the software HSC Chemistry 9®. The partial pressure of SiO(g) (p_{SiO}) is known from Reaction (1). Assuming that the gas is ideal, the activity and the partial pressures are equal. Activity of solid silica is assumed to be 1. Therefore, p_{O2} can be found from

$$K_{eq} = \frac{1}{(p_{SiO})^2 \, p_{O_2}}$$

If we compare this work with Hu et al., we can conclude that oxygen may not be the cause of stacking faults in this work. However, the authors cannot claim that defects are hardly generated because of low oxygen content. Hu et al.'s work does not document presence of oxygen defects either, but it just assumes that oxygen partial pressure is high enough (p_{O2} = 10^{-3}) to generate defects. Growth of SiC often results into stacking faults and amorphous domains for silicon carbide, regardless of the growing environment. [3,29–32].

The second step of the mechanism takes place at the high interface energy points, as proposed by Wu et al. [12]. The continuous SiO_x layer changes its shape to the bead structures. The main assumption of this theory is that SiO_x is liquid, and that it can move around thanks to the surface repulsion with SiC. Therefore, another assumption is that liquid SiO_x has a low wettability towards SiC. If there was a high wettability, a uniform layer would still be present. The fluidity of SiO_x is a very good point of the BTL mechanism [12]. SiO_x is assumed to have the same melting point and phase transition points of silica.

Temperatures at which beads are noticed are well below the melting point of SiO_x. There can be two explanations to this fact. First, the reaction between SiO(g) and CO(g) is strongly exothermic ($\Delta H^{(-1)}_{1700°C}$ = -1406 kJ/mol). A local increase in temperature can lead to softening or melting of silica. Secondly, the nanosized system is affected by the melting point depression effect, typical of systems in the order of magnitude of 10-100 nanometers [33]. Previous works on nanowires growth show the same configurations at temperatures well below the melting point of silica [8,10,23]. In particular, Liu et al. [10] clearly state that SiO_x is a liquid reassembled into spherical nanodroplets. Nanowires generated below 1500°C in experiments by Liu et al., whereas silica melts at 1710°C, according to HSC Chemistry 9®.

The beads generated mostly in the region where the concentration of stacking faults and twins in the wires is high, or where the wires cross their ways. When nanowires cross their paths, SiO_x nodules will be able to merge. By doing so, the shell phase will further reduce its energy. Higher temperatures should increase the formation of nodules at the crossing paths, whereas bead structures are more common at lower temperatures. The results from this work shows that nodules can form almost on every kind of nanowire, from the most defect-free to the richest in stacking faults. Some naked nanowires rich in stacking faults were also found. Finally, SiO_x can move and create even larger beads, by merging nodules from different nanowires.

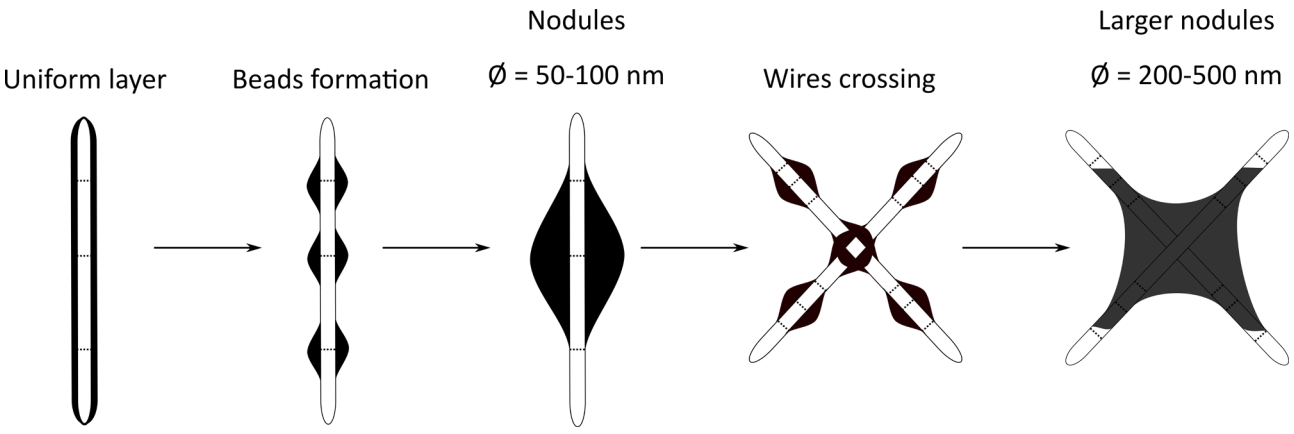

Fig. 9: Beads formation mechanism, revised after [12]. White = solid SiC; Black = Liquid SiO_x; Dotted lines = stacking faults

Contact angle. The contact angle remains in the same range of values, regardless the temperature reached. The angle will vary until the gas-liquid-solid interface system reaches the interfacial energy balance conditions. The interfaces obey the Young's law, until the interface

energy of the active site (e.g. a stacking fault or an oxygen inclusion in SiC) is compensated. Further interface energy reduction can occur by increasing the nodule size.

The contact angle varies between 0° and 45±10°. The lower limit corresponds to the uniform coating, and the higher to the nodules and beads configurations. Parameters controlling the contact angle are not easy to control. One can enhance the formation of nodules by exposing the nanowires at high temperatures, to decrease the viscosity of SiO_x. In fact, the viscosity of silica is depending on temperature. On the other hand, uniform coatings or naked nanowires are favored by a slow nanowire growth, an oxygen-free environment, low exposure times and temperatures. In this way, the nanowires will be poor in stacking faults.

The transition from a continuous to a bead structure is depending on the local microstructure and energy balance. SEM analyses show that the continuous layer structure is preferred below 1200-1250°C, while the bead structure is often found above this temperature interval. Nanowires showing different structures can be found in the same area. For example, Figures 3 and 6 show nanowires containing both nodules and continuous layer structures.

It will be very difficult to control the formation of the SiO_x layer, as temperatures varies locally at nanoscale. The number of defects in the core-phase plays a major role in the early stages of nodule formation. However, the wettability and exposure times at high temperature define the final microstructure. Monocrystalline SiC core-phases should be nodules-free according to the proposed mechanism, because of the low wettability. However, uncoated wires can also be rich in stacking faults, since liquid SiO_x could flow away in the latest nodule formation stages.

Further comments on previous theories on nodule formation. The proposed mechanism was built after the considerations stated by two works. The first is the study carried out by Wu et al. [12]. It was seen that many valid assumptions were made in this mechanism, despite it works in the opposite way to the one proposed in this study (i.e. beads are formed initially, then making layers). For example, Wu proposed the viscosity change of SiO_x and the formation of nodules at the crossing points of nanowires. These two issues were not discussed in Liu's work.

There is a contradiction in the BTL mechanism by Wu et al. [12]. The authors state that there should be a good wettability between SiO_x and SiC. Good wettability means high chances of noticing uniform layers embedding the nanowires. However, bead structures are noticed also where interface energy was high, for example in the presence of defects. This fact was noticed not only in this work, but also in Wu et al. and Liu et al. [10]. The formation of bead structure is influenced by stacking faults only at early stages. It is believed that SiO_x and SiC have bad wettability at nanoscale, as supported by Liu et al. [10]. One should not forget as well that the amount of each phase influences the wettability. It could also be that the nodules are generated by excessive amount of SiO_x in the same area.

The mechanism proposed by Liu et al. [10] is a LTB-type, as the one proposed in this work. The mechanism is coherent with the mass balance, as the shell-phase and the core-phase are generated at the same time. This also fits good with the Oxide-Assisted Growth theory by Noor Mohammad [33]. The theory was proposed to explain the structure of core-shell nanowires of different composition, especially for silicon-containing species. The chemistry and thermodynamics of this mechanism will be covered in a future work [28].

Conclusion

The formation of nodules in SiC-SiO_x nanowires is a dynamic process. Below the melting point depression temperature, SiO_x will cover SiC with a thin, uniform layer. When exposed to high temperatures, the uniform layer transforms into a bead-structured composite nanowire. Beads formation occurs at stacking faults. Here the higher surface energy acts as a driving force for the shape variation process.

Adjacent nodules will further reduce their surface energy by increasing their contact area with the SiC core-phase. This can be done in two ways. One alternative is to agglomerate into larger

beads, giving life to bead structures and nodules. The other is to adhere to more than one SiC-nanowire, especially where nanotreads nearly cross their paths.

Holding time dependence would be a meaningful result to discuss the formation mechanism. Further analysis of samples should be performed at different holding times, to evaluate the kinetics of transformation of the nodules.

Acknowledgments

The TEM work was carried out using NORTEM infrastructure, Grant 197405, TEM Gemini Centre, Norwegian University of Science and Technology (NTNU), Norway. The authors would like to thank Ragnhild Sæterli (NTNU) for the collaboration in the TEM analysis. The present study was supported by Elkem AS and the EnergiX program of the Research Council of Norway through project 269431 SiNoCO2.

References

[1] Y. Zhang, C.A. Pickles, J. Cameron, The production and mechanical properties of silicon carbide and alumina whisker-reinforced epoxy composites, J. Reinf. Plast. Compos. 11 (1992) 1176–1186.

[2] A. Meng, Z. Li, J. Zhang, L. Gao, H. Li, Synthesis and Raman scattering of b-SiC/SiO2 core-shell nanowires, J. Cryst. Growth. 308 (2007) 263–268.

[3] Z. Li, W. Gao, A. Meng, Z. Geng, L. Gao, Large-Scale Synthesis and Raman and Photoluminescence Properties of Single Crystalline b-SiC Nanowires Periodically Wrapped by Amorphous SiO2 Nanospheres 2, J. Phys. Chem. 113 (2009) 91–96.

[4] X.J. Wang, J.F. Tian, L.H. Bao, C. Hui, T.Z. Yang, C.M. Shen, H.-J. Gao, F. Liu, N.S. Xu, Large Scale SiC/SiOx nanocables: Synthesis, photluminescence, and field emission properties, J. Appl. Phys. 102 (2007) 1–6.

[5] J. Wang, S. Liu, T. Ding, S. Huang, C. Qian, Synthesis, characterization and photoluminescence properties of bulk-quantity β-SiC/SiOx coaxial nanowires, Mater. Chem. Phys. 135 (2012) 1005–1011.

[6] S.C. Dhanalaban, M. Negri, F. Rossi, G. Attolini, M. Campanini, F. Fabbri, M. Bosi, G. Salviati, Effects of growth parameters on SiC/SiO2 core/shell nanowires radial structures, Mater. Sci. Forum. 740–742 (2013) 494–497.

[7] B. Zhong, L. Kong, B. Zhang, Y. Yu, L. Xia, Fabrication of novel hydrophobic SiC/SiO2 bead-string like core-shell nanochains via a facile catalyst/template-free thermal chemical vapor deposition process, Mater. Chem. Phys. 217 (2018) 111–116.

[8] P. Hu, S. Dong, K. Gui, X. Deng, X. Zhang, Ultra-long SiC nanowires synthesized by a simple method, R. Soc. Chem. 5 (2015) 66403–66408.

[9] P. Hu, R.-Q. Pan, S. Dong, K. Jin, X. Zhang, Several millimeters long SiC-SiOx nanowires synthesized by carbon black and silica sol, Ceram. Int. 42 (2016) 3625–3630.

[10] H. Liu, Z. Huang, J. Huang, M. Fang, Y.-G. Liu, X. Wu, Thermal evaporation synthesis of SiC/SiOx nanochain heterojunctions and their photoluminescence properties, J. Mater. Chem. C. 2 (2014) 7761–7767. https://doi.org/10.1039/c4tc01391c.

[11] J. Wei, K.-Z. Li, H.-J. Li, Q.-G. Fu, L. Zhang, Growth and Morphology of one-dimensional SiC nanostructures without catalyst assistant, Mater. Chem. Phys. 95 (2006) 140–144.

[12] R. Wu, B. Zha, L. Wang, K. Zhou, Y. Pan, Core-shell SiC/SiO2 Heterostructures in nanowires, Phys. Status Solidi A. 209 (2012) 553–558. https://doi.org/10.1002/pssa.201127459.

[13] P. Kang, B. Zhang, G. Wu, H. Gou, Synthesis of SiO2 covered SiC nanowires with milled Si,C nanopowders, Mater. Lett. 65 (2011) 3461–3464.

[14] J.-S. Lee, Y.-K. Byeun, S.-H. Lee, S.-C. Choi, In situ growth of SiC nanowires by carbothermal reduction using a mixture of low-purity SiO2 and carbon, J. Alloys Compd. 456 (2008) 257–263.

[15] J.-M. Qian, J.-P. Wang, G.-J. Qiao, Z.-H. Jin, Preparation of porous SiC cercamic with a woodlike microstructure by sol-gel and carbothermal reduction processing, J. Eur. Ceram. Soc. 24 (2004) 3251–3259.
[16] H. Huang, J.T. Fox, F.S. Cannon, S. Komarneni, In situ growth of silicon carbide nanowires from anthractie surfaces, Ceram. Int. 37 (2011) 1063–1072.
[17] G.W. Meng, L.D. Zhang, C.M. Mo, S.Y. Zhang, H.J. Li, Y. Qin, S.P. Feng, Synthesis of One-Dimensional Nanostructures-b-SiC nanorods with and without amorphous SiO2 wrapping layers, Metall. Mater. Trans. A. 30A (1999) 213–219.
[18] H. Mølnås, Investigation of SiO-condensate formation in the silicon process, NTNU, Trondheim, Norway, 2010.
[19] J. Vangskåsen, Metal-producing reactions in the Carbothermic Silicon process, Master thesis, NTNU, Department of Materials Science and Engineering, 2012.
[20] M.S. Khrushchev, Kinetics and Mechanism of Reaction between Silicon Carbide and Silica, Inorg. Mater. 36 (2000) 462–464.
[21] M. Ksiazek, I. Kero, Challenging in transporting the off-gases from the Silicon process, in: Takano Int. Symp. Met. Alloys, 2015: pp. 157–166.
[22] A. Broggi, M. Tangstad, E. Ringdalen, Small scale experiments simulating condensation of SiO and CO in silicon production, in: Silicon Chem. Sol. Ind. XIV, Svolvær, Norway, 2018: pp. 139–152.
[23] Y. Hu, X. Liu, X. Zhang, N. Wan, D. Pan, X. Li, Y. Bai, W. Zhang, Bead-curtain shaped SiC@SiO2 core-shell nanowires with superior electrocheical properties for lithium-ion batteries, Electrochem. Acta. 190 (2016) 33–39.
[24] C.A. Pickles, J.M. Toguri, The Plasma Arc production of Si-based ceramic whiskers, J. Mater. Res. 8 (1992) 1996–2003.
[25] W.-S. Seo, K. Koumoto, Stacking faults in b-SiC formed during carbothermal reduction of SiO2, J. Am. Ceram. Soc. 79 (1996) 1777–1782.
[26] A. Broggi, M. Tangstad, E. Ringdalen, Characterization of Si-SiO2 mixture generated from SiO and CO, Metall. Mater. Trans. B. 50 (2019) 2667–2680. https://doi.org/10.1007/s11663-019-01678-x.
[27] Thermal Technology LLC, Operating and Maintenance Instructions - Model# 1000-3560-FP20, (2012).
[28] A. Broggi, E. Ringdalen, M. Tangstad, Characterization, thermodynamics and mechanism of reaction of nanowires produced from SiO(g) and CO(g) (to be published), (2020).
[29] S.R. Nutt, Defects in silicon carbide whiskers, J. Am. Ceram. Soc. 67 (1984) 428–431.
[30] G. Cheng, T.-H. Chang, Q. Qin, H. Huang, Y. Zhu, Mechanical Properties of Silicon Carbide Nanowires: Effect of Size-Dependent Defect Density, Nano Lett. 14 (2014) 754–758.
[31] S. Chen, W. Li, X. Li, W. Yang, One-dimensional SiC nanostructures: Designed growth, properties, and applications, Prog. Mater. Sci. 104 (2019) 138–214.
[32] M. Bechelany, A. Brioude, D. Cornu, G. Ferro, P. Miele, A Raman Spectroscopy Study of Individual SiC Nanowires, Adv. Funct. Mater. 17 (2007) 939–943.
[33] S. Noor Mohammad, Investigation of the oxide-assisted growth mechanism for nanowire growth and a model for this mechanism, J. Vac. Sci. Technol. B. 26 (2008) 1993–2007.
[34] A. Schei, J. Tuset, H. Tveit, Production of high Silicon Alloys, 1st ed., Tapir, Trondheim, Norway, 1998.
[35] S. Stølen, T. Grande, Chemical Thermodynamics of Materials: Macroscopic and Microscopic Aspects, 1st ed., John Wiley & Sons, 2004.